Optimized Design Of Holddown Springs With Bending Leaves

Dr Bérenger d'Uston - FRAMATOME ANP - Nuclear Fuel - Lyon - France

ABSTRACT

The function of the holddown springs is to guarantee the axial holddown of the fuel assemblies throughout their in-reactor operation up to their final unloading.

In order to minimise the height of the top nozzle on which they are mounted, these springs are made up of a stack of bending leaves whose tilt guarantees the necessary stroke to accomodate the gap variations between the top of the assemblies and the upper core plate.

Given the required holddown forces and the available space, the spring leaves undergo plastic strains in normal service during the vessel closure and cold return phases. Analyses of the stresses and strains in the leaf material is necessary to rule out the risks raised by such loadings under PWR conditions. A dedicated computational tool is used to conduct these analyses; this module integrates the following non-linear behaviour models:

- large displacements and rotations,
- elastic-plastic strains,
- one-sided contacts with sliding and friction.

This software enables rapid simulation of the behaviour of leaf springs in the preliminary design phase, and analysis of the loadings experienced by the material. With this tool, spring geometry can be optimized by minimizing the stresses and plastic strains on the material, while maintaining the required level of holddown force.

1. INTRODUCTION

Axial holddown of the fuel assemblies is required for all the operating conditions, from the moment the assemblies are placed in the core and a coolant flow passes through them. Holddown counteracts the liftoff of the bottom nozzle from the lower core plate to limit the amplitude of the flow-induced vibrations and to minimize any resulting wear.

Axial holddown is generally provided by a spring pack mounted on the top nozzle. The space available at this location is conditioned by accessibility to the assembly gripping zones, the presence of the RCCA spider, and the search for the largest fuel stack length, which leads to the total top nozzle height being limited.

The solution with the best compactness is indisputably the one with springs made up of a stack of bending leaves (fig 1). In addition to its compactness, this system features a number of advantages; its fabrication is relatively simple, it only needs one screw and one tapping in the top nozzle for attachment and it does not feature any mechanical joint liable to seize up in service.

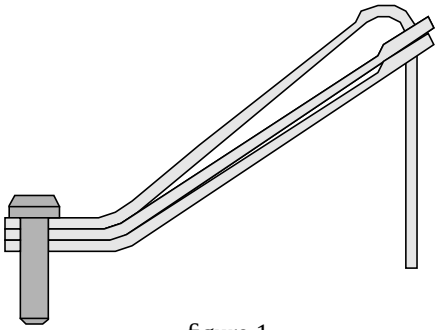

figure 1

This system must be able to accommodate variations in the gap between the top of the assembly and the upper core plate. This gap depends not only on the relevant operating conditions (cold shutdown, at-power operation), but also on the growth of the assembly and therefore on its burnup.

Its capacity for plastic accommodation is an advantage with respect to the latter condition, as it confers on the holddown system a behaviour with little dependence on assembly burnup. This drastically reduces the risks of assembly bowing at end of life. The use of materials in an elastic-plastic strain range raises a number of questions which are not addressed by the codes setting the design rules and which need to be analyzed to verify the integrity of these components in operation.

A simplified model of the leaf springs is given in §2. With this model, numeric simulations can be made of the operation of these components to evaluate their performance and the material loading level can be estimated. The main phenomena that occur during deformation of the leaf springs require the following non-linear behaviours to be taken into account:

- large displacements and rotations,
- elastic-plastic strains,
- one-sided contacts with sliding and friction.

A dedicated software called RIGIDE includes these models, two applications of this software are presented in §3. A calculation model corresponding to a real spring is used to simulate several cycles of compression that have been applied to this spring during tests. It is also shown how the design of a holddown spring can be improved with respect to in-service mechanical strength, while maintaining the required level of holddown force and simplifying the fabrication of the component.

2. MECHANICAL MODEL OF THE HOLDDOWN SPRINGS

2 . 1 Approach Adopted for Large-Displacement and Large-Rotation Beam Elements

Given their geometries and their connection and loading modes, the bending leaf springs are modelled in their plane of symmetry by assuming plane stress behaviour.

Deformation of the spring leaves results in a transformation of their geometry such that it is no longer possible to consider the usual hypotheses on infinitesimal displacements as valid. The most obvious effect is the significant variation in moment arm (horizontal projection of the distance from the fixed end to the point of application of the axial forces), which is a major factor in the calculation of bending moments.

The approach adopted is to take as mechanical system parameters the local deformation state of each of the discretization elements. Each leaf is divided into a succession of beam elements and each of the elements in this chain structure is clamped to the end section of its preceding element and deforms according to the modes of a fixed-free beam (fig 2).

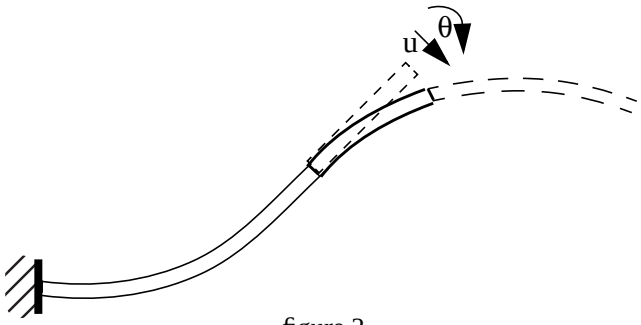

figure 2

The degrees of freedom of an element (u, θ), are respectively the transverse displacement and the rotation of the free end of this element, expressed in the coordinate frame for its fixed section. The set of degrees of freedom of all the leaf discretization elements forms the vector of the generalized variables (q). The overall mechanical equilibrium is described by the virtual work principle by considering the applied loads ($\overline{F}_a$) and the stress distribution in the leaves (σ):

$$\frac{\partial}{\partial q}\left\langle \overline{F}_a \cdot \delta\overline{v} - \int_V (\sigma \cdot \delta\varepsilon)\, dV \right\rangle = 0 \qquad (1)$$

where δ denotes a kinematically allowable virtual variation of the following quantity,
$\overline{v}$ is the displacement of the points of application of the external or connecting forces,
ε represents the local strain field in the leaves.

The non-linearity inherent in large-displacement and large-rotation structures is taken into account by reconstituting the deformed geometry of each leaf, which conditions the projection of the applied loads:

$$\bar{F}_a \cdot \delta\bar{v} \;=\; \bar{F}_a \cdot \frac{\partial}{\partial q}\bar{v} \cdot \delta q \tag{2}$$

This operation involves updating the position and orientation of the free end of each of the elements, allowing for the position and orientation of the end section of its preceding element in the chain structure and its own bending deformation. These updates are performed sequentially by following the order of description of the chain structure.

This parameter-setting is particularly effective for springs made up of bending leaves, as the leaves can be considered, at least initially, as a set of independent cantilever beams. If the discretization of the beams is dense enough, the resulting elongation of the leaves is negligible, even under the effect of pronounced bending.

2 . 2 Elastic-Plastic Strains

Tests run on holddown springs show that for deflections representative of in-reactor operation, particularly at the time of vessel closure, significant permanent deformation remains after load relaxation. This residual deflection shows that the material of the spring leaves (generally Inconel 718) undergoes stresses greater than its yield strength.

Credit must be taken for this phenomenon, as the behaviour of a spring after yielding is obviously different from what it was before. To take this phenomenon into account, the material tensile curve needs to be applied over a sufficiently wide strain range.

The calculation hypotheses generally acknowledged in elastic beam theory postulate that the stresses and strains vary linearly across the thickness and that they are proportional, for each point, to its distance from the mid-fiber if the beam works in pure bending. This study only considers the kinematic side of these hypotheses; only strains vary linearly across the thickness. It is further considered that the shear strains generated by shearing forces induce negligible deflections compared with those due to bending (slender beam hypothesis).

In these conditions, the reduction elements of the load set exerted at the free end of a fixed-free beam are obtained as follows: two individual sections are analyzed (fig 3); these are respectively located in the first and last quarter of the length of the considered element.

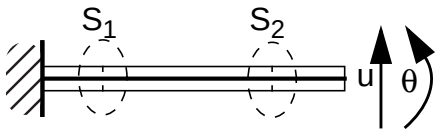

figure 3

Cubic interpolation functions are used to calculate the local curvature induced by deformation (i.e. second derivative of the transverse displacement w relative to axial position s) in each of these sections. Each section features a dozen integration points spread across the thickness (fig. 4), total strain is calculated at each of these points:

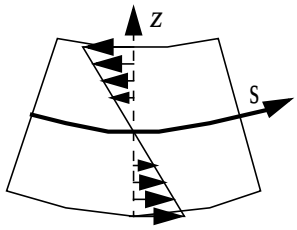

figure 4

$$\varepsilon_t \;=\; -z \cdot \frac{d^2 w}{ds^2} \tag{3}$$

The local stresses are then obtained by taking into account the material stress-strain curve and the plastic strains already experienced during previous deformations (ε_p):

$$\sigma = \sigma_{ep}(\varepsilon_t, \varepsilon_p) \tag{4}$$

These local stresses are integrated using a discrete method which gives the resulting bending moment in the rectangular section of width *b* and thickness *h*:

$$M = b \cdot \int_{-h/2}^{h/2} -z \cdot \sigma(z) dz \tag{5}$$

The transport relationships of the bending moment in each of the two sections make it possible to determine the shearing force *S* and torque *T* exerted at the free end of the element which form the vector of internal forces *F(q)*.

2 . 3 One-sided Contacts with Sliding and Friction

The leaves making up a spring cannot be considered as independent whenever the compression of the spring induces multiple contacts between its components. To be representative, the calculation model must take into account these interactions between leaves; the Lagrange multiplier method is particularly suitable for taking into account the conditions for non-interpenetration of contacting solids.

The first step must be to list all the contact possibilities liable to occur between the leaves and with the environment. Once this list has been made, the kinematics of each of the potential contacts must be characterized; four different kinds of 2D contact are revealed, of which three are illustrated in figure 5:

- contact between the seating zone (tang) of the upper leaf and the upper core plate (1) is governed by a circle/straight line kinematics,
- contact between the top leaf and the first counterleaf (2) is governed by a point/straight line kinematics,
- contacts between the ends, assumed non-deformable, of the adjacent counterleaves (3) are governed by a segment/straight line kinematics,
- interferences liable to occur between the leaves in their flexible portions are governed by a curve/curve kinematics.

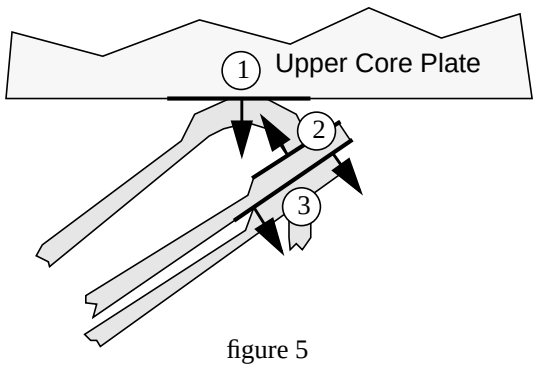

figure 5

Considering that a segment/straight line or curve/curve type contact can be reduced to a set of point/straight line type contacts, only two kinds of contact remain to be allowed for.

Application of the Lagrange multiplier method starts with the expression of the non-interpenetration relationships which, for any condition *i* can be written as:

$$G_i(q) \leq 0 \tag{6}$$

The partial derivation of these quantities from the generalized variables gives the coefficients of the constraint equations for the non-interpenetration relationships:

$$B_n(i,j) = -\frac{\partial}{\partial q_j} G_i(q) \tag{7}$$

Matrix B_n thus defined can also be interpreted as the operator projecting the normal forces of the contacts on the mechanical system degrees of freedom. By following the same approach, a matrix B_t is defined as being the operator projecting tangent forces (friction) on the mechanical system degrees of freedom.

This matrix is combined with the previous one according to the following expression:

$$B_c(i,j) = B_n(i,j) + (\pm\mu_i) \cdot B_t(i,j) \tag{8}$$

where μ_i is the friction coefficient of the materials pair involved in contact i

This gives the projection operator of the contact forces which are exerted in either of the directions delimiting the friction cone on the mechanical system degrees of freedom.

The friction coefficient is given a sign which depends on the change in the loading applied to the spring. The tangent direction which conditions the operator B_t is conventionally defined so that during a spring compression phase the friction coefficient is a positive factor in Eq 8 and a negative one in an unloading phase.

Considering that the loading/unloading of a spring is obtained by vertical displacement of the upper core plate relative to the base of this spring, the latter does not sustain any external force, but is subjected, through the contact with the upper core plate, to an imposed deflection (Eq 6). Then, the mechanical equilibrium of a spring is fully described by the following expression:

$$[B_c]^t\{\lambda\} - F(q) = 0 \tag{9}$$

where B_c represents the matrix of the contact equations with friction established in Eq 8,
λ represents the vector of Lagrange multipliers; these forces are necessary to meet the non-interpenetration conditions for the established contacts,
$F(q)$ represents the vector of internal forces as calculated in §2.2

The unknowns of the problem are therefore the generalized variables (q) and the Lagrange multipliers (λ) assigned to all the potential contacts. The simulation of compression cycles is carried out by applying the loading step by step. The mechanical equilibrium is found at each step by an iterative method. At each iteration, the next calculation steps (Eq 10 to 13) are carried out:

$$\Delta q = [S]^{-1}\left\{ [B_c]^t\{\lambda\} - F(q) \right\} \tag{10}$$

$$\Delta\lambda = \left[[B_n][S]^{-1}[B_c]^t \right]^{-1}\left\{ G(q) - [B_n]\{\Delta q\} \right\} \tag{11}$$

$$q = q + \Delta q + [S]^{-1}[B_c]^t\Delta\lambda \tag{12}$$

$$\lambda = \lambda + \Delta\lambda \tag{13}$$

where :

$$S(i,j) = \frac{\partial}{\partial q_j} F_i(q) \tag{14}$$

This sequence solves all the non-linear equations for the leaves (Eq 10), while taking into account the non-linear kinematic relationships (Eq 11), which exist between these leaves.

Control of the appearance or disappearance of the contacts is facilitated by specifically addressing the Lagrange multipliers (Eq 11). For each established contact, these multipliers represent the normal component of the interaction force between the involved solids. The activation of a non-established contact is triggered by a positive value of G (Eq 6). The deactivation of an established contact is triggered by a negative value of its associated multiplier λ.

Only sliding situations are addressed for established contacts; the sticking phenomena which would lead to the whole friction cone and not just its limits being considered are unlikely owing to the imposed-deformation loading mode.

3. APPLICATIONS

3 . 1 Validation of the Numerical Simulation Tool

The RIGIDE software applies the modelling techniques presented in § 2. It relies upon the design methods already in use and adds to them. The software user inputs in a data deck the material properties and the dimensioning of the springs as it appears on the fabrication and inspection drawings. The discretization and description of the potential contacts are carried out by the software.

In preliminary design, the model generally takes into account nominal dimensions. However, it is possible with this tool to take into account the actual dimensions of a fabricated spring and to compare the calculation results with those obtained during characterization tests.

The software qualification was demonstrated by carrying out this type of comparison for 40 cases, corresponding to 8 different designs. Figure 6 presents the calculation results obtained by simulating the 5 successive compression cycles which were applied in the test to a real spring and the corresponding experimental results.

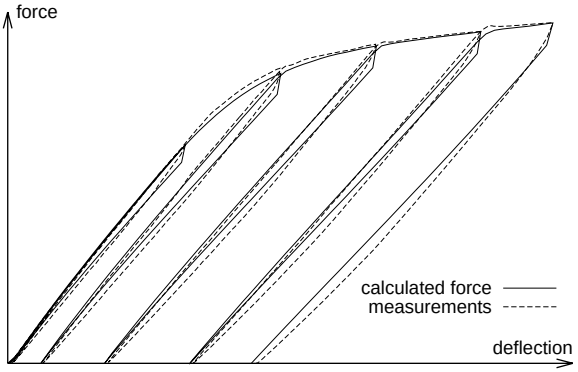

4 leaves AFA 3GL spring : force vs deflection

figure 6

Model representativity must be assessed not only by considering the values of the developed forces at the maximum deflections of the applied cycles, but also by comparing the residual deflection values obtained by test and by calculation at the end of each of the cycles.

The small deviations which occur between the calculated and measured curves during the spring unloading phases are attributable to the friction model. This model takes no account of the transient sticking state of the contacts, which occurs during reversal of upper core plate motion. Considering that in reactor conditions these sticking phenomena are eliminated by assembly vibrations, the friction model is representative.

The geometry of the calculated spring, reduced to the mid-fiber and to the contour of the end of each leaf, is presented in figure 7 for two extreme configurations corresponding to the non-deformed state and to the deformation shape under maximum deflection.

The straight line segment which appears between the continuous sections of the upper leaf and the first counterleaf marks the location of an interference between these two leaves. This interference was observed during the tests on all the springs of this design. Such an interference is only acceptable if it occurs sufficiently far from the fixed end of the leaves; otherwise, it would reveal a problem of mutual geometrical incompatibility of the leaves.

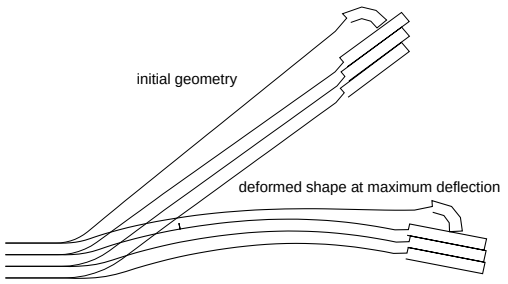

4 leaves AFA 3GL spring : initial and deformed shapes

figure 7

3 . 2 Optimization of Spring Design

Given the relevance of the results obtained during simulation, this tool was used to conduct a study for optimizing the shape of the springs of the type presented in the previous section. The aim of the optimization is to minimize the plastic strain rate at the base of the upper leaf, while maintaining the performance level of the original design.

On the basis of the additional data supplied by these calculations, the level and distribution of the bending moments in each leaf can be estimated with high accuracy. Starting from these data, the next step is to find the bending inertia spread which best matches the bending moment, at least in the most stressed zones.

In their original design, the leaves are machined across the thickness so that their bending inertia decreases from the fixed end to the free end. This machining is performed by milling, so it can only produce an inclined plane. The bending inertia depends on the cube of the thickness, so a linearly varying inertia cannot be obtained by this means.

The proposed solution is to keep a constant thickness and to reduce, in the same ratio as the bending moment, the leaf width to which the inertia is directly proportional. The results of this optimization are presented in figure 8, which shows the plastic strain trend profiles in the upper leaf skin of the analyzed spring, before and after shape optimization. It can be observed that the maximum plastic strain rate which is localized at the spring fixed end is reduced by a factor 2, with no impact on the overall performance of the spring.

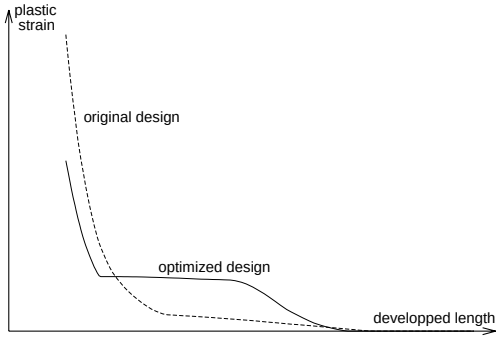

4 leaves AFA 3GL spring : top leaf shape optimization

figure 8

4. CONCLUSION

The design tool built on the basis of the development work outlined here-above was used to analyze the behaviour of the holddown leaf springs and to control their stress and strain condition. It is a valuable aid in shortening the design cycle of these components and ruling out any risk of malfunction. It also helps to find new spring geometries matching the required performance levels, while minimizing plastic strains.